AIAA SciTech Forum
January 3-7, 2022, San Diego, CA & Virtual
AIAA SCITECH 2022 Forum

10.2514/6.2022-2566

Inlet Diffusor Buoyancy – Its Historical Use in Supersonic Transport Design

Bhargav Chaudhari [1]
and
Timothy T. Takahashi[2]
Arizona State University, Tempe, Arizona, 85287

This paper presents the significance of inlet buoyancy thrust on the net thrust of a turbojet engine, especially in the supersonic region. The work presented in this paper illustrates the difference in the values obtained from considering the inlet buoyancy thrust and the classical 1-D thrust equation, which often tends to neglect the impact of change in pressures in the capture area through the fan face of the engine when compared along with real flight performance value as advertised by General Electric for GE4/J4C turbojet engine which was supposed to be implemented on the Boeing 2707-100 SST. This paper includes a complete turbojet engine analysis based on 1-D thrust equation along with a simpler buoyancy force estimation.

I. Introduction

SUPERSONIC TRANSPORT AIRCRAFT have beguiled the general public, the airlines and engineers for more than half a century. Press releases by Gulfstream [1], Aerion [2], and Boom Aerospace [3] document the continued effort to develop some sort of replacement for the BaE Concorde, the world's only successful supersonic transport which flew its last revenue flight in 2003. [4] Professor Takahashi and his students have been equally interested in the promise of resurgence of commercial supersonics and have worked a number of propulsion and airframe design studies over the past few years.

An efficient propulsion system is an essential component of a successful long-range aircraft. The engines need to produce sufficient thrust to overcome drag under engine-inoperative conditions at takeoff, climb and accelerate to cruise altitude and efficiently sustain steady-level high-altitude, high-speed flight. Thus, to design a supersonic aircraft, engineers need to access accurate and precise propulsion data at the earliest conceptual design stages.

Prior AIAA conference papers document how Professor Takahashi's students labored to produce quality "five-column" installed propulsion performance data for generic supersonic aircraft from widely available, unclassified sources. In prior work published by Dickman & Takahashi [5], Palma & Takahashi [6] and Cleary & Takahashi [7], we married the thermodynamic and momentum-propulsive predictions from NPSS [8] to an inlet loss model found in PIPSI. [9][10][11][12] Dickman [5] modelled a supersonic engine/inlet system with a fixed geometry normal shock inlet feeding a low-bypass-ratio turbofan. Palma [6] tried a fixed-geometry external compression inlet feeding a low-bypass-ratio turbofan. Cleary [7] extended Palma's work [6] to try to look at higher-bypass-ratio engines and determine the optimal schedule of a "bypass door" to actively trade spillage-drag and bypass-drag for "optimal" installed performance.

In these earlier studies, we found relatively disappointing installed performance at high speeds – ram drag effects quickly diminish the installed thrust – leading to engines dependent upon afterburners to provide sufficient thrust for

[1] M.S. Candidate, Aerospace Engineering, Arizona State University, P.O. Box 876106, Tempe, AZ. Member AIAA.
[2] Professor of Practice, Aerospace Engineering, Arizona State University, P.O. Box 876106, Tempe, AZ. Associate Fellow AIAA.

high-speed / high-altitude cruise. A lack of implied "super-cruise" capability radically restricts the range of a supersonic aircraft, rendering it commercial unviable.

Professor Takahashi began to suspect that that our poor predicted performance was due to mathematical oversight. His inspiration came from a lay article describing the propulsion system of the BaE Concorde. [13][14] On Concorde, the engine is mounted behind a complex variable geometry intake. A movable ramp system provides subsonic flow to the engine face at all flight conditions; see Fig. 1. While the physical dimensions of the inlet capture area and the engine fan face remain constant, the movable ramps define a system with a variable throat area.

This article stated that "at takeoff and during subsonic flight, 82% of the thrust is developed by the engine alone with 6% from the nozzles and 21% from the intakes." [13][14] It also claims that during supersonic cruise "8% of the power is derived by the engine with the other 29% being from Nozzles and an impressive 63% from the intakes." [13]

Professor Takahashi found this statement inspiring; that "intake thrust" was not some byproduct of trapped shock waves in an internal compression supersonic inlet, but a broad phenomenon seen across a wide speed range. He then realized that forces due to pressurization of the inlets were not accounted for in classic 1-D propulsion analysis; precisely the methods defined with NPSS [8] and PIPSI [9][10][11][12]

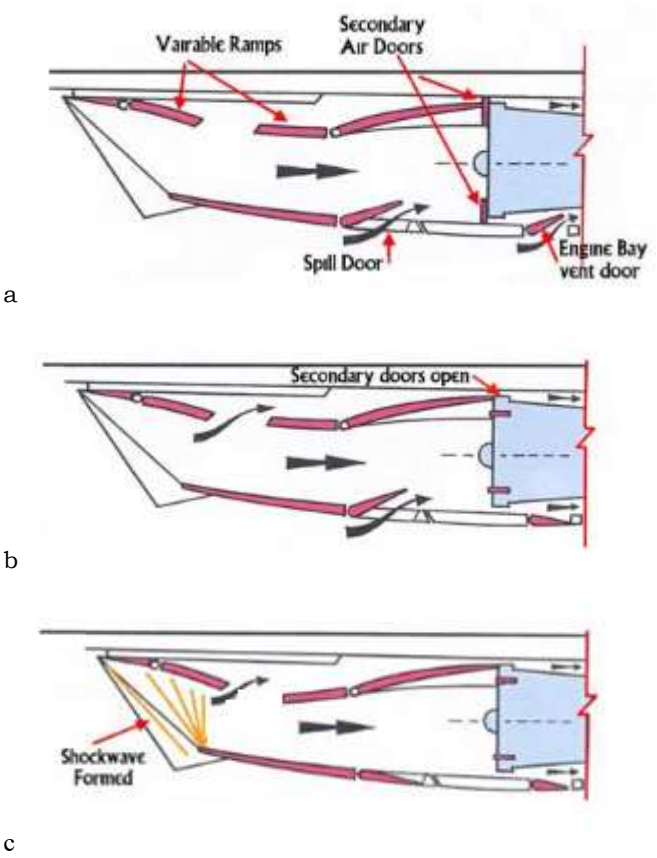

Fig. 1 – Schematic of the Variable Ramp External Compression Inlet System of the BaE Concorde [13]

Takahashi & Cleary [15] in 2020 declared that the axial force developed by propulsive airflow entering the airframe can be called out as **inlet buoyancy**. This term-of-art describes the net pressure-thrust developed by the flow within the confines on the inlet duct. As the flow slows from high speeds to a relatively low speed at the fan face it trades dynamic pressure for static pressure. When the airframe designer configures the inlet as a net diffusor (with a smaller entrance area than engine fan area), static pressure increases as flow moves downstream through the duct. This axial pressure gradient is akin to "wind tunnel buoyancy" forces due to boundary layer and wake blockage that are seen during external flow experiments. The net pressure difference between the duct throat and engine fan face acts upon the projected axial surface area of the inlet and transmits a force to the airframe. The static pressurization of the duct attempts to expel the duct forwards, "spitting" it off the front face of the engine. Thus, an inlet diffusor can produce a propulsion system related force that opposes drag.

With a very simple 1-D compressible flow analysis, Takahashi & Cleary [15] estimated the magnitude of this inlet buoyancy force for a variety of subsonic and supersonic inlets and found the rough-order-of-magnitude of these forces consistent with the description found in that lay article on Concorde [13]. In this new work, Chaudhari & Takahashi document reasons for us to believe that inlet buoyancy forces were properly accounted for the installed propulsion model of the GE4/J4C supersonic turbojet engine intended to propel the Boeing B2707-100 SST. While a description of this vital component of installed thrust eluded openly published reports [9][10][11][12] and classic texts [16], it was well known within the propulsion community in the 1950's and 60's.

II. Force Accounting

When an engine is installed in an "air vehicle," its performance requires the engineer to account for various parasitic drag contributions (positive or negative!); this is a tricky "book-keeping" problem. Historically, engineers have lumped thrust and drag contributions together in different ways; this inconsistency makes this a muddy subject. Keith Numbers [17] describes force accounting as "the procedure by which the air vehicle components and the forces that act on them are defined and categorized as either **aerodynamic** or **propulsion** related." Each discipline (aerodynamics or propulsion) must determine the forces and moments on their assigned components.

On a conventional airplane, it seems that the inlet, engine, and nozzle are distinctly separate from the basic airframe. Numbers [17] holds that "since the aerodynamic and propulsion components have little influence on each other, the aerodynamicist and propulsion analyst can conduct independent assessments easily." We can see evidence of this in Fig. 2; a high-speed wind-tunnel test installation for aerodynamic performance / stability / control assessment of the Lockheed A-12 "Blackbird." We note the presence of hollow, flow-through inlets, completely lacking the famous spike. Absent these features, forces and moments measured here (and incorporated into the aerodynamic database) cannot capture the impact of the elaborate shock structure which develops around the real inlet.

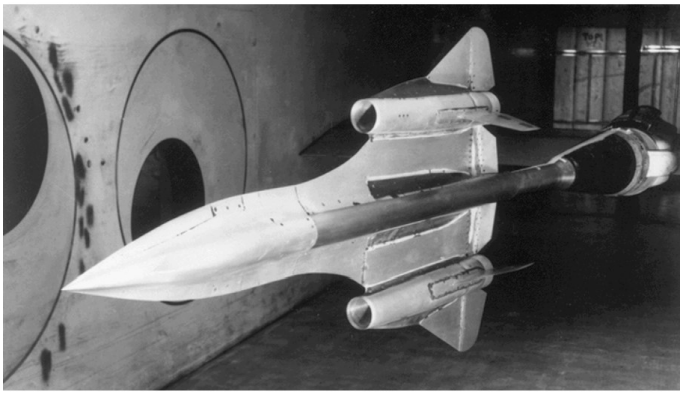

Fig. 2 – Lockheed A-12 High-Speed Wind Tunnel Model (installed in the NASA/Ames 8x8-ft Unitary Plan Wind Tunnel)

Numbers [17] was very aware of this bifurcation in responsibility. He called forth that engineers must specify two force accounting interfaces: one for the separation of propulsion and aerodynamic surfaces and another for the engine control volume boundaries. [17] The Aero-Propulsion Interface (API) separates surfaces that lead to forces and moments in the aerodynamic model (lift, drag, pitching moment, etc.) from those which enter the propulsion model ("five-column-data" of thrust and thrust-specific-fuel consumption as a function of speed, altitude and power-lever-angle). The Engine-Airframe Interface (EAI) is the control volume associated with the model that engineers use to deduce "uninstalled thrust" (the classical zero through nine propulsion stream-tube reference station nomenclature). Engineers use a 1-D aero/thermodynamic representation (such as that represented with an NPSS model) because a direct integration of pressure and shear stress on moving internal engine components is impractical.

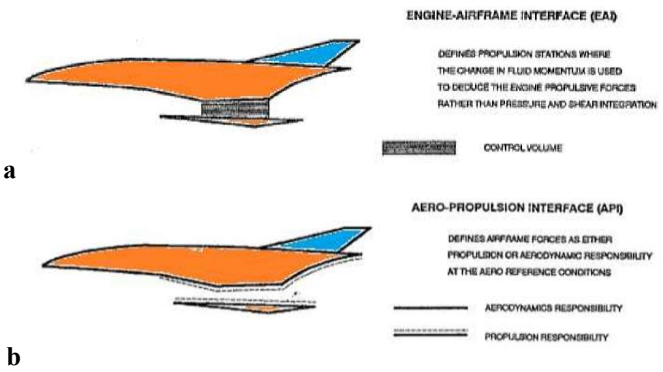

Fig. 3 – Numbers [17] call for the need for dual simultaneous force accounting standards.

Numbers holds that the "EAI can be considered the portion of the propulsion system forces which are supplied by the engine company." [17] Thus, NPSS "provides cycle decks, tabular data, or thrust stand data in the form of net engine forces between the EAI boundaries." [17] Numbers reiterates that the "API defines the entire propulsion system, and the EAI defines that portion of the propulsion system which is provided by the engine company;" thus installed performance must not neglect the forces unique to the API. [17]

On an aircraft like the Concorde, the Boeing 2707-100 (see Fig. 4) or the Lockheed A-12/SR-71, engineers commonly apply the "free-stream-to-tail" accounting system. In Fig. 5, we see the surfaces wetted by the propulsion airflow that will be bookkept with propulsion colored BLUE and the remainder of the airframe which will be bookkept with aerodynamics colored RED. In addition, Numbers reminds us that there are cross influences from the propulsion system acting upon aerodynamic surfaces; for example, "engine airflow throttling and propulsion system variable geometry, which can change forebody shock structures … (or) exhaust flow influence on trimming surfaces in the tail region." [17]

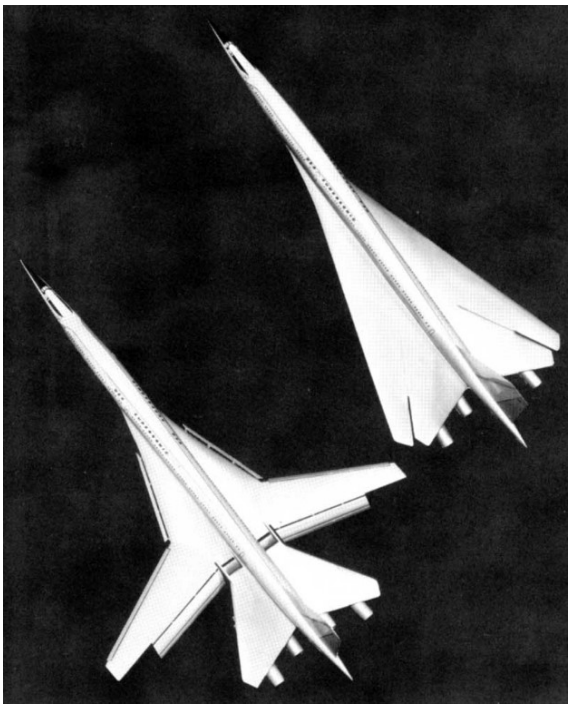

Fig. 4 – Conceptual Models of the Boeing B2707-100 Supersonic Transport

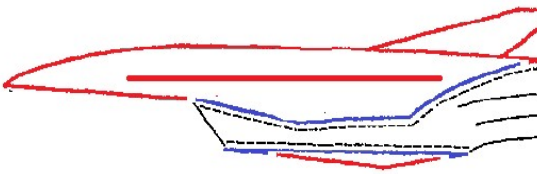

Fig. 5 – Typical Free-Stream-To-Tail Force Accounting System (after Numbers [17])

III. The GE-4 Turbojet Engine proposed for the B2707-100

In this work, we seek to confirm to advertised performance of the General Electric's GE4/J4C turbojet engine proposed for incorporation onto the Boeing B2707-100 Supersonic Transport. [18] In doing so, we realize that we must implement an inlet buoyancy thrust correction above and beyond the results we would otherwise obtain using the classical 1-D thrust estimation method to match published performance data.

The GE4/J4C turbojet engine is a lightweight, high performance engine with augmented support highly optimized for supersonic use. It was the only passenger jet engine with an afterburner. It was designed with the primary aim of achieving higher supersonic speeds of Mach 2.5 to Mach 3. It can reach a maximum speed of Mach 3 and sustain flight at 80,000 feet. [21]

The basis for this engine derives from the YJ93 turbojet engine (also known as GE-3) used on the North American XB-70 Valkyrie. Most of the data related to GE4/J4C turbojet engine model stays confidential till date and hence remains inaccessible. However, we have found a document describing the GE4/J5P turbojet engine. [25]

The GE4/J5P has length of approximately 27 ft 4 inches with diameter of 5 ft 11 inches. It had a nine-stage axial compressors with an overall pressure ratio of 12.5:1 and

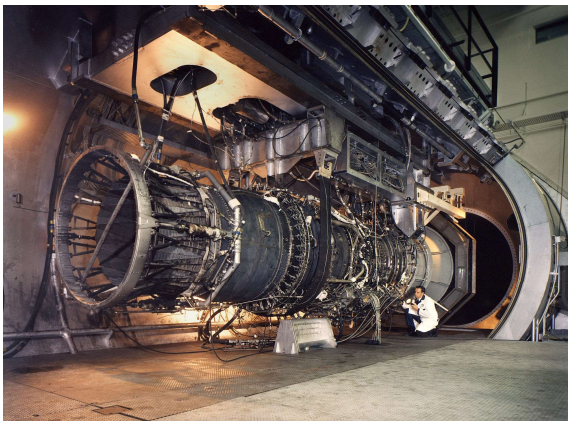

Fig. 6 – Photograph of a GE4 engine in a test cell

inlet face diameter of 60.6 inches, and an annular straight-through-flow combustor. The two-stage axial turbines with turbine inlet temperature of 1204 ºC were aligned with exhaust nozzle with diameter of 74.2 inches. [25]

In this work, we use the available geometric and key engine design parameters to successfully validate the performance of this turbojet engine. Here, we document the significance of accounting for inlet diffusor buoyancy across the full flight-envelope: from static conditions to extreme flight speed limit of engine at Mach 3 and 75,000-ft.

IV. GE4/J4C Turbojet Engine Propulsion Database

An installed propulsion "five-column-data" database is a wide collection of net thrust and specific fuel consumption values at different power lever angle (PLA) settings, Mach numbers and altitudes.

The flight performance curves are depicted below in Fig. 7 and Fig. 8 show net thrust, and specific fuel consumption as a function of engine power setting and Mach number of the flight. These performance values were measured at Sea Level, 15,000-ft, 25,000-ft, 36,089-ft, 45,000-ft, 55,000-ft, 65,000-ft, and 75,000-ft altitude range. In our digitization of the published data, we retain General Electric's definition of power-code; see Table 1.

Table 1 Power-Lever-Angle Nomenclature

Power Setting Name	*G.E. Power Setting Number*
Maximum thrust, augmented	1
Partial augmentation	2
Partial augmentation	3
Minimum thrust, augmented	4
Mid power thrust	-
Maximum thrust, non-augmented	5
95% engine RPM	7
85% engine RPM	9
75% engine RPM	11

The General Electric report [21] ostensibly provides us with data based on the 1962 U.S. Standard Atmosphere [22] with no bleed or power extraction, fuel conforming to G. E. Commercial Jet Fuel. Specification A50T27A and follows MIL-E-5008B [23] standard for ram recovery which states that, ram recovery is 1 up to sonic speed, after which it reduces as a function of Mach number of the flight.

In a companion paper, [24] we utilized this data, in conjunction with a first-principles estimate of aerodynamic lift and drag properties, to document the mission performance of the B2707-100.

The net thrust and thrust specific fuel consumption (TSFC) values as published in the General Electric's GE4/J4C engine performance report is presented below in Figs 7 & 8 at a wide variety of speeds and altitudes. [21] After digitizing the data, we sorted and reformatted this data into "square" "full-factorial" tables suitable for interpolation in our point-performance and mission-performance codes.

The performance report papers published during the development of SST used a General Electric engine and performance of the same GE4/J4C engine which has a relatively vague description of its performance basis [21]. The engine never saw installation on the B2707 aircraft since it was never developed. Most of the data is extrapolated from flight on a subsonic B-52 and the supersonic XB-70; a YJ93 not a GE4/J4C engine.

The XB-70 as mentioned above, used the YJ93-GE-3 engine, for which some data is available online, including the single-spool design, 11-stage compressor and 2-stage turbine, turbine inlet temperature of 2560ºR (1422 ºK)at max thrust, inlet air mass flow rate of 275-lbm/s (125 kg/s) at max thrust, and max thrust of 22,000-lbf (98 kN) without afterburner and 29,250-lbf (130 kN) with afterburner.[21] The key missing piece is the OPR at max thrust, which still

remains uncertain at this point. Having the OPR would help perform a turbojet flow path analysis with assumed values of component efficiencies based on the vintage of the engine. However, there are other engines from which one can draw reasonable then-state-of-the-art component efficiencies. Although the power hook curves look consistent with other engine performance data available from the time, it still remains very important to relate the values and check for its plausibility.

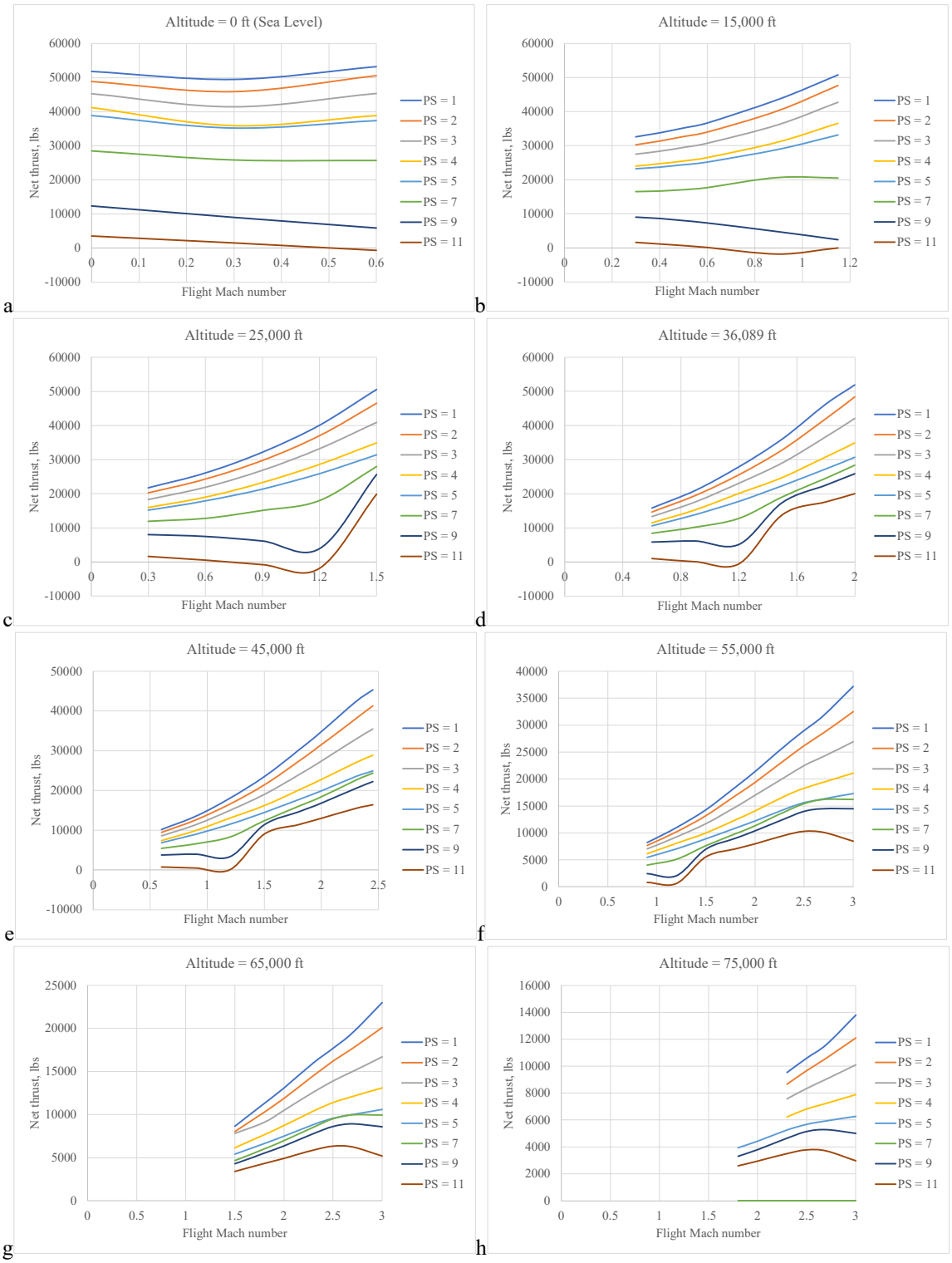

Fig. 7 – GE4/J4C Engine Installed Thrust Data across the flight envelope (after [21])

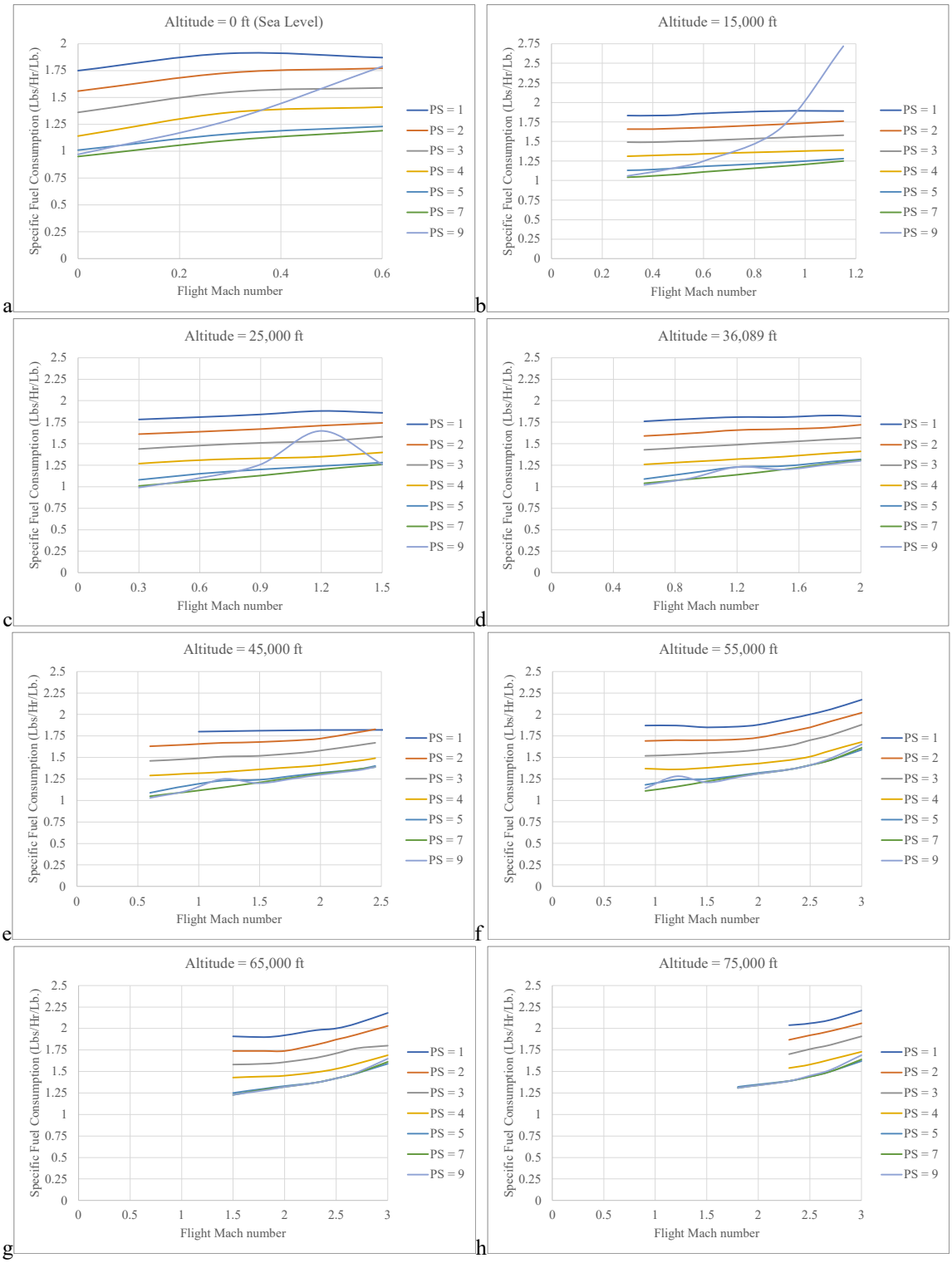

Fig. 8 – GE4/J4C Engine Thrust-Specific-Fuel-Consumption Data across the flight envelope (after [21])

V. Methodology to Validate GE's Installed Propulsion Performance

To better understand the basis of this data, we developed a generic turbojet engine analysis to estimate the thrust and specific fuel consumption data presented in the GE report. [21] Where possible we used the same parameters as openly published; this set is incomplete, as we had to reverse engineer other confidential or unspecified parameters in order to complete our analysis.

The available data for GE-4 engine contains the standard atmosphere data from 1962 since it was the one used in propulsion calculation [22]. This would mean an input data block would be ready for inlet/diffusor condition for analysis. Along with this it was specifically stated that the GE4 engine would have 12.5:1 overall pressure ratio [23]. Hence, this pressure ratio has been split up based on the fact that having equal compression would provide consistent and better result.

The other parts of the engine were mostly the component efficiencies which would be used for turbojet flow-path analysis. The data for this still remains unclear for GE-4 engine. However, one could use the data of other engines from the same era on the internet at different sources. It is not unusual for legacy engines like this GE-4 to have poor characterization in online sources, and much of what is online might actually be wrong. So, it becomes important to do some real sleuthing to get decent numbers. There are many amazing engines from that era that can be used for reference.

Yet, one need to understand and acknowledge the fact that engines use the then-available state-of-the-art values in terms of Turbine Inlet Temperature (TIT), Static Pressure Ratio (SPR), and component efficiencies. Most of the data used for this turbojet analysis is based on several engine references such as YJ93-GE3 and P&W J58 engine. Based on Paul H. Wilkinson as mentioned in his book [25], the diameters of compressor inlet and exhaust nozzle for the GE-4 engine are 60.6 inches and 74.2 inches, respectively.

The data for geometry and working of inlet and the conical spike are not available for general public use. As a result, several part of this had to be reverse engineered based on the data available and other engine references. A supersonic axisymmetric spike was developed to understand and develop the inlet performance chart. For this purpose, a reference variable geometry translating axisymmetric spike was studied which was implemented on SR-71 [26].

Based on this data available and considering other important aspect which could be reverse engineered such as diffusion ratio from back tracking the design condition Mach number after series of conical shocks followed by a normal shock, a conical axisymmetric spike for supersonic inlet was designed. The pressure recovery for which is displayed in the Figure 9 below along with just the standard normal shock pressure recovery which occurs on an unstarted inlet for a series of Mach numbers [27].

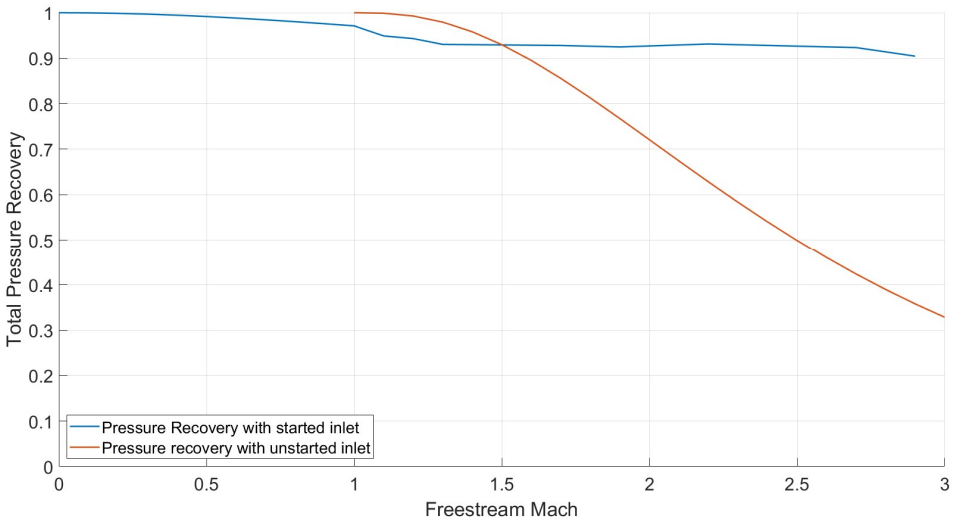

Fig. 9 – Pressure Recovery comparison for started and unstarted inlet

In this work, we performed a complete turbojet engine analysis to develop data which will help legitimize the published GE4 report values [21]. Based on concepts of air-breathing propulsion system estimations; the jet, and pressure thrusts were calculated using several combinations of thermodynamic equations involved in each stage and its relationship with the next stage. The data was obtained using a temperature limited Brayton cycle analysis for non-ideal condition.

VI. Propulsion Analysis

The core turbojet analysis we ultimately coded in MATLAB. It utilizes the concepts of air – breathing propulsion taught by Prof. Dahm in his Aircraft Propulsion class at Arizona State University [28]; refer to Fig. 10. The final simplified equations are mentioned below. It must be noted that before using the analysis tool, a thorough understanding of each components is essential to provide inputs such as Mach numbers, dimensions, and efficiencies of each component to account for irreversibility associated with engine. The data for freestream conditions must be selected from the standard atmosphere table to get consistent results to that observed in engine performance charts.

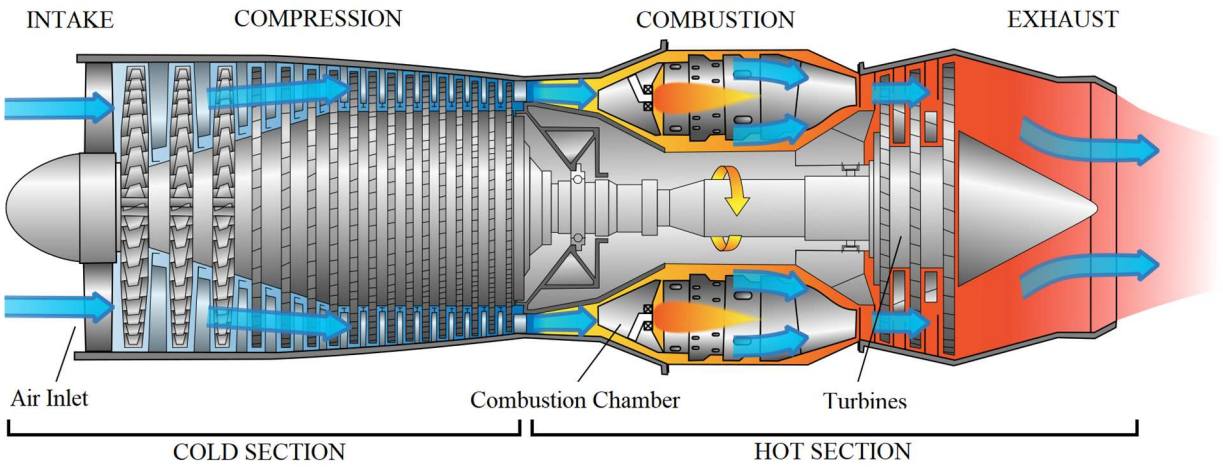

Fig. 10 – Sectional Representation of a Turbojet engine

Inlet / Diffuser Section

$$T_{t_{inlet}} = T_{t_{freestream}} \quad \textit{Eq. 1}$$

$$P_{t_{inlet}} = P_{t_{freestream}} \cdot \left[\frac{1 + \eta_d \frac{(\gamma - 1)}{2} M_{freestream}{}^2}{1 + \frac{(\gamma - 1)}{2} M_{freestream}{}^2} \right]^{\frac{\gamma}{\gamma - 1}} \quad \textit{Eq. 2}$$

$$T_{inlet} = \frac{T_{t_{inlet}}}{\left[1 + \frac{(\gamma - 1)}{2} M_{inlet}{}^2 \right]} \quad \textit{Eq. 3}$$

$$P_{inlet} = \frac{P_{t_{inlet}}}{\left[1 + \frac{(\gamma - 1)}{2} M_{inlet}{}^2 \right]^{\frac{\gamma}{\gamma - 1}}} \quad \textit{Eq. 4}$$

Fan Section

$$P_{t_{fan}} = (Fan\ Pressure\ Ratio)\ .\ P_{t_{inlet}} \quad \textit{Eq. 5}$$

$$T_{t_{fan}} = T_{t_{inlet}} \cdot \left\{ 1 + \frac{1}{\eta_{fan}} \left[\left(\frac{P_{t_{fan}}}{P_{t_{inlet}}} \right)^{\frac{\gamma}{\gamma - 1}} - 1 \right] \right\} \quad \textit{Eq. 6}$$

$$T_{fan} = \frac{T_{t_{fan}}}{\left[1 + \frac{(\gamma - 1)}{2} M_{fan}{}^2 \right]} \quad \textit{Eq. 7}$$

$$P_{fan} = \frac{P_{t_{fan}}}{\left[1 + \frac{(\gamma - 1)}{2} M_{fan}{}^2\right]^{\frac{\gamma}{\gamma-1}}} \quad \textit{Eq. 8}$$

$$|w_{fan}| = C_{p\,\gamma\to 1.4}\left[T_{t_{fan}} - T_{t_{inlet}}\right] \quad \textit{Eq. 9}$$

Low Pressure Compressor (LPC) Section

$$P_{t_{LPC}} = (Pressure\ Ratio_{LPC}) \,.\, P_{t_{fan}} \quad \textit{Eq. 10}$$

$$T_{t_{LPC}} = T_{t_{fan}} \cdot \left\{1 + \frac{1}{\eta_{LPC}}\left[\left(\frac{P_{t_{LPC}}}{P_{t_{fan}}}\right)^{\frac{\gamma}{\gamma-1}} - 1\right]\right\} \quad \textit{Eq. 11}$$

$$T_{LPC} = \frac{T_{t_{LPC}}}{\left[1 + \frac{(\gamma - 1)}{2} M_{LPC}{}^2\right]} \quad \textit{Eq. 12}$$

$$P_{LPC} = \frac{P_{t_{LPC}}}{\left[1 + \frac{(\gamma - 1)}{2} M_{LPC}{}^2\right]^{\frac{\gamma}{\gamma-1}}} \quad \textit{Eq. 13}$$

$$|w_{LPC}| = C_{p\,\gamma\to 1.4}\left[T_{t_{LPC}} - T_{t_{fan}}\right] \quad \textit{Eq. 14}$$

High Pressure Compressor (HPC) Section

$$P_{t_{HPC}} = (Pressure\ Ratio_{HPC}) \,.\, P_{t_{LPC}} \quad \textit{Eq. 15}$$

$$T_{t_{HPC}} = T_{t_{LPC}} \cdot \left\{1 + \frac{1}{\eta_{HPC}}\left[\left(\frac{P_{t_{HPC}}}{P_{t_{LPC}}}\right)^{\frac{\gamma}{\gamma-1}} - 1\right]\right\} \quad \textit{Eq. 16}$$

$$T_{HPC} = \frac{T_{t_{HPC}}}{\left[1 + \frac{(\gamma - 1)}{2} M_{HPC}{}^2\right]} \quad \textit{Eq. 17}$$

$$P_{HPC} = \frac{P_{t_{HPC}}}{\left[1 + \frac{(\gamma - 1)}{2} M_{HPC}{}^2\right]^{\frac{\gamma}{\gamma-1}}} \quad \textit{Eq. 18}$$

$$|w_{HPC}| = C_{p\,\gamma\to 1.4}\left[T_{t_{HPC}} - T_{t_{LPC}}\right] \quad \textit{Eq. 19}$$

Combustor Section

$$P_{Combustor} = P_{HPC} \quad \textit{Eq. 20}$$

$$T_{t_{Combustor}} = T_{Combustor} \cdot \left[1 + \frac{(\gamma - 1)}{2} M_{Combustor}{}^2\right] \quad \textit{Eq. 21}$$

$$P_{t_{Combustor}} = P_{Combustor} \cdot \left[1 + \frac{(\gamma - 1)}{2} M_{Combustor}{}^2\right]^{\frac{\gamma}{\gamma-1}} \quad \textit{Eq. 22}$$

$$|q_{Combustor}| = C_{p\,\gamma\to 1.3}\left[T_{t_{Combustor}} - T_{t_{HPC}}\right] \quad \textit{Eq. 23}$$

High Pressure Turbine (HPT) Section

$$|w_{HPT}| = |w_{HPC}| \quad \textit{Eq. 24}$$

$$T_{t_{HPT}} = T_{t_{Combustor}} - \frac{|w_{HPT}|}{C_{p\,\gamma\to 1.3}} \quad \textit{Eq. 25}$$

$$P_{t_{HPT}} = P_{t_{Combustor}} \cdot \left[1 - \frac{1}{\eta_{HPT}}\left(1 - \frac{T_{t_{HPT}}}{T_{t_{Combustor}}}\right)\right]^{\frac{\gamma}{\gamma-1}} \quad \textit{Eq. 26}$$

$$T_{HPT} = \frac{T_{t_{HPT}}}{\left[1 + \frac{(\gamma - 1)}{2} M_{HPT}{}^2\right]} \quad \textit{Eq. 27}$$

$$P_{HPT} = \frac{P_{t_{HPT}}}{\left[1 + \frac{(\gamma - 1)}{2} M_{HPT}{}^2\right]^{\frac{\gamma}{\gamma-1}}} \quad \textit{Eq. 28}$$

Low Pressure Turbine (LPT) Section

$$|\dot{W}_{LPT}| = |\dot{W}_{LPC}| + |\dot{W}_{fan}| \quad \textit{Eq. 29}$$

$$|w_{LPT}| = |w_{LPC}| + [1 + BPR].|w_{fan}| \quad \textit{Eq. 30}$$

$$T_{t_{LPT}} = T_{t_{HPT}} - \frac{|w_{LPT}|}{C_{p_{\gamma \to 1.3}}} \quad \textit{Eq. 31}$$

$$P_{t_{LPT}} = P_{t_{HPT}} \cdot \left[1 - \frac{1}{\eta_{LPT}}\left(1 - \frac{T_{t_{LPT}}}{T_{t_{HPT}}}\right)\right]^{\frac{\gamma}{\gamma-1}} \quad \textit{Eq. 32}$$

$$T_{LPT} = \frac{T_{t_{LPT}}}{\left[1 + \frac{(\gamma - 1)}{2} M_{LPT}{}^2\right]} \quad \textit{Eq. 33}$$

$$P_{LPT} = \frac{P_{t_{LPT}}}{\left[1 + \frac{(\gamma - 1)}{2} M_{LPT}{}^2\right]^{\frac{\gamma}{\gamma-1}}} \quad \textit{Eq. 34}$$

Converging Nozzle Section

$$\text{Choking Check, } M' = \sqrt{\frac{2}{(\gamma-1)} \cdot \frac{\eta_{nozzle} \cdot \left[1 - \left({}^{P_{freestream}}/_{P_{LPT}}\right)^{\frac{\gamma}{\gamma-1}}\right]}{1 - \eta_{nozzle} \cdot \left[1 - \left({}^{P_{freestream}}/_{P_{LPT}}\right)^{\frac{\gamma}{\gamma-1}}\right]}} \quad \textit{Eq. 35}$$

If $M' > 1$ i.e., Choked Nozzle

$$M_{exit} = 1 \quad \textit{Eq. 36}$$

$$T_{t_{exit}} = T_{t_{LPT}} \quad \textit{Eq. 37}$$

$$P_{exit} = P_{t_{LPT}} \cdot \left\{\left[1 - \frac{1}{\eta_{nozzle}}\left(\frac{\gamma - 1}{\gamma + 1}\right)\right]^{\frac{\gamma}{\gamma-1}}\right\} \quad \textit{Eq. 38}$$

$$T_{exit} = \frac{T_{t_{exit}}}{\left[1 + \frac{(\gamma - 1)}{2} M_{exit}{}^2\right]} \quad \textit{Eq. 39}$$

$$P_{t_{exit}} = P_{exit} \cdot \left[1 + \frac{(\gamma - 1)}{2} M_{exit}{}^2\right]^{\frac{\gamma}{\gamma-1}} \quad \textit{Eq. 40}$$

Else $M' \leq 1$ i.e., Unchoked Nozzle

$$M_{exit} = M' \quad \textit{Eq. 41}$$

$$T_{t_{exit}} = T_{t_{LPT}} \quad \textit{Eq. 42}$$

$$P_{exit} = P_{freestream} \quad \textit{Eq. 43}$$

$$T_{exit} = \frac{T_{t_{exit}}}{\left[1 + \frac{(\gamma - 1)}{2} M_{exit}{}^2\right]} \quad \textit{Eq. 44}$$

$$P_{t_{exit}} = P_{exit} \cdot \left[1 + \frac{(\gamma - 1)}{2} M_{exit}{}^2\right]^{\frac{\gamma}{\gamma-1}} \quad \textit{Eq. 45}$$

Thrust Estimation

$$V_{exit} = M_{exit} \cdot \sqrt{\gamma R T_{exit}} \quad \textit{Eq. 46}$$

$$\dot{m}_{exit} = \frac{P_{exit}}{R\,T_{exit}} \cdot V_{exit} \cdot A_{nozzle} \quad \textit{Eq. 47}$$

Rocket Thrust, $F_{Rocket} = \dot{m}_{exit} \cdot V_{exit}$ *Eq. 48*

Ram Drag, $F_{Ram-Drag} = -\dot{m}_{exit} \cdot V_{freestream}$ *Eq. 49*

Pressure Thrust, $F_{Pressure} = \left(P_{exit} - P_{freestream}\right) \cdot A_{nozzle}$ *Eq. 50*

Now, to calculate the aerodynamic force due to high pressure changes in inlet section, we need to estimate inlet buoyancy force.

Inlet Buoyancy Thrust as explained in the inlet buoyancy thrust estimation paper [15] by Takahashi & is,

$$F_{Buoyancy} \approx \left[\frac{1}{2}\left(P_{throat} + P_{cowl}\right) - P_{shock}\right]\left(A_{cowl} - A_{throat}\right) + \left[\frac{1}{2}\left(P_{fan} + P_{throat}\right) - P_{shock}\right]\left(A_{fan} - A_{throat}\right) \quad \textit{Eq. 51}$$

where, P_{shock} is the static pressure at upstream flow of the inlet where, in the case of flight at supersonic speeds, a normal or oblique or conical shockwave may form. At subsonic speeds, flow conditions do not change here. To visually understand where this points are located, the inlet flow path analysis has been displayed in Fig. 11, 12 and 13, which illustrates the nomenclature used in buoyancy force estimation under different conditions of incoming freestream.

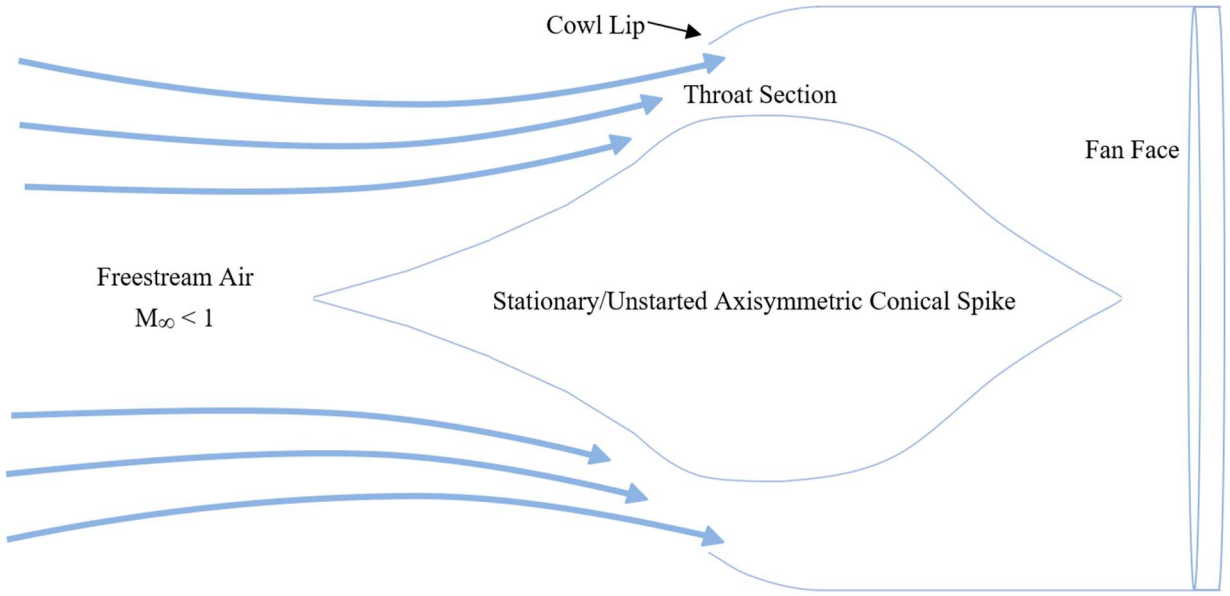

Fig. 11 – Schematics of Axisymmetric Conical Spike Inlet Section under Purely Subsonic Freestream Condition

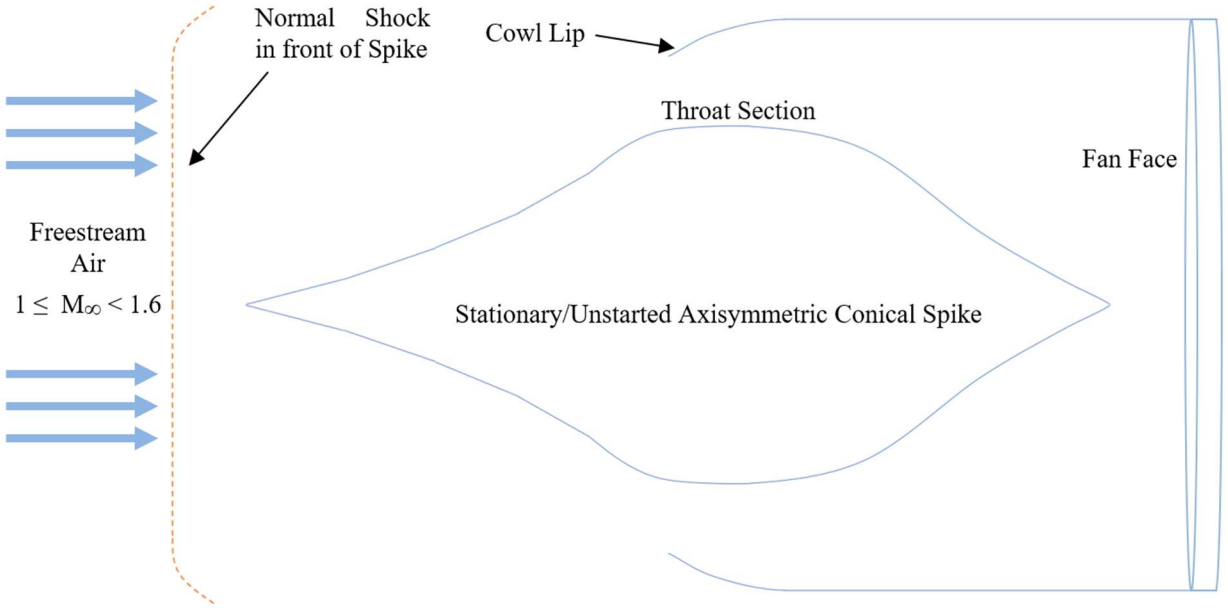

Fig. 12 – Schematics of an Unstarted Axisymmetric Conical Spike Inlet Section at Lower Supersonic Freestream Condition

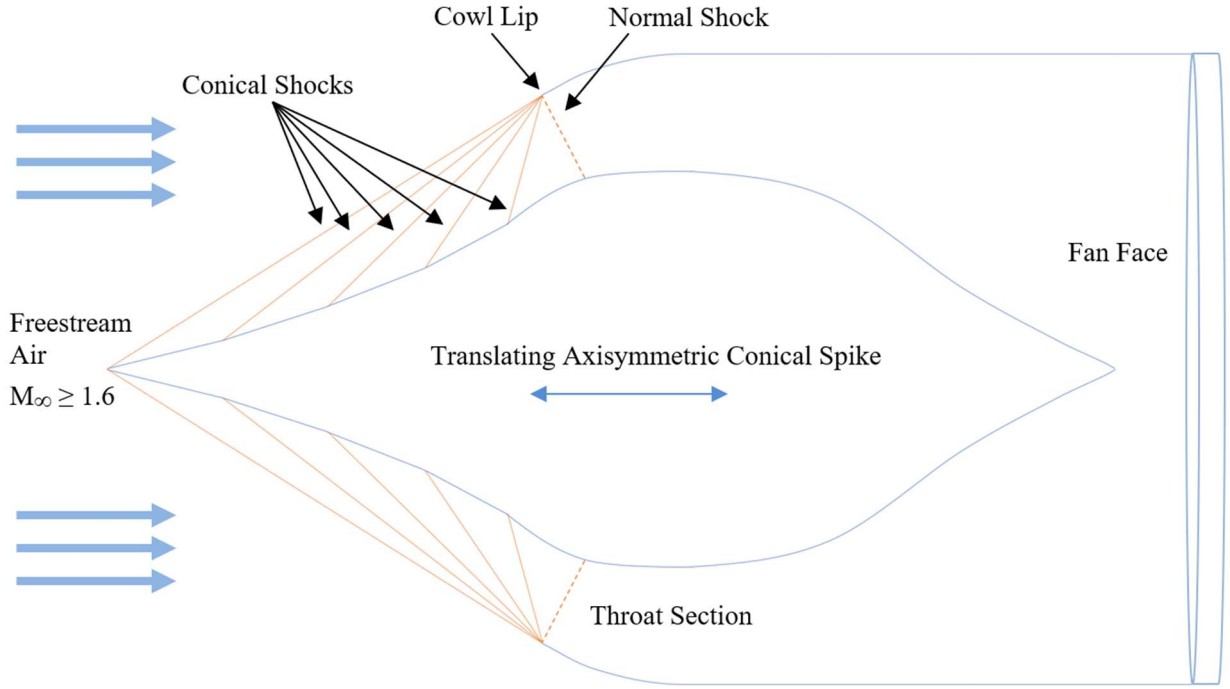

Fig. 13 – Schematics of Started Axisymmetric Conical Spike Inlet Section at Higher Supersonic Freestream Condition

The inlet buoyancy term used here is not part of the classic air breathing propulsion equation, but it is an additional term which is essential to account for the huge pressure difference thrust that is generated at higher Mach number in the inlet. Hence it becomes necessary to add such quantity while estimating the thrust of the entire system. This term falls under the aerodynamics side of the thrust estimation. The Net thrust can be estimated in the following way.

Net Thrust, $F_{Net} = F_{Ram-Drag} + F_{Rocket} + F_{Pressure} + F_{Buoyancy}$ *Eq. 52*

VII. Results

Upon using the above mentioned method, the MATLAB solver was ran at altitude of 0 ft, 15000 ft, 25000 ft, 36089 ft, 45000 ft, 55000 ft, 65000 ft, and 75000 ft to obtain the results at reference conditions mentioned in GE4/J4C report. This results have been compared at Military thrust condition (Non-Augmented Maximum Thrust), since the data for rest of the setup at partial and augmented conditions were not available. A total of 46 different points were used for calculating and comparing the military thrust to understand the impact of buoyancy thrust on propulsion performance of an engine.

The net thrust value (F_N) as obtained from calculating jet, pressure and inlet buoyancy force and net thrust presented in the performance report published by the General Electric's Flight Propulsion Division for GE4/J4C turbojet engine are displayed below. Every alternate figures from Fig. 13 through 29 compares the military thrust values at each test altitude and using the values at Mach number given in published report without applying any complex regression method to alter the readings in between. The three values compared are for published thrust value in the GE report, newly estimated thrust upon considering the effects of buoyancy, and classical 1-D thrust equation without considering the buoyancy effects.

The figure succeeding the comparison figure illustrates the component-wise distribution of thrust at different Mach numbers at reference altitude. The thrust here has been presented into split values of Ram Drag, Rocket Thrust, Pressure Thrust, Buoyancy Thrust and Net Thrust (F_N).

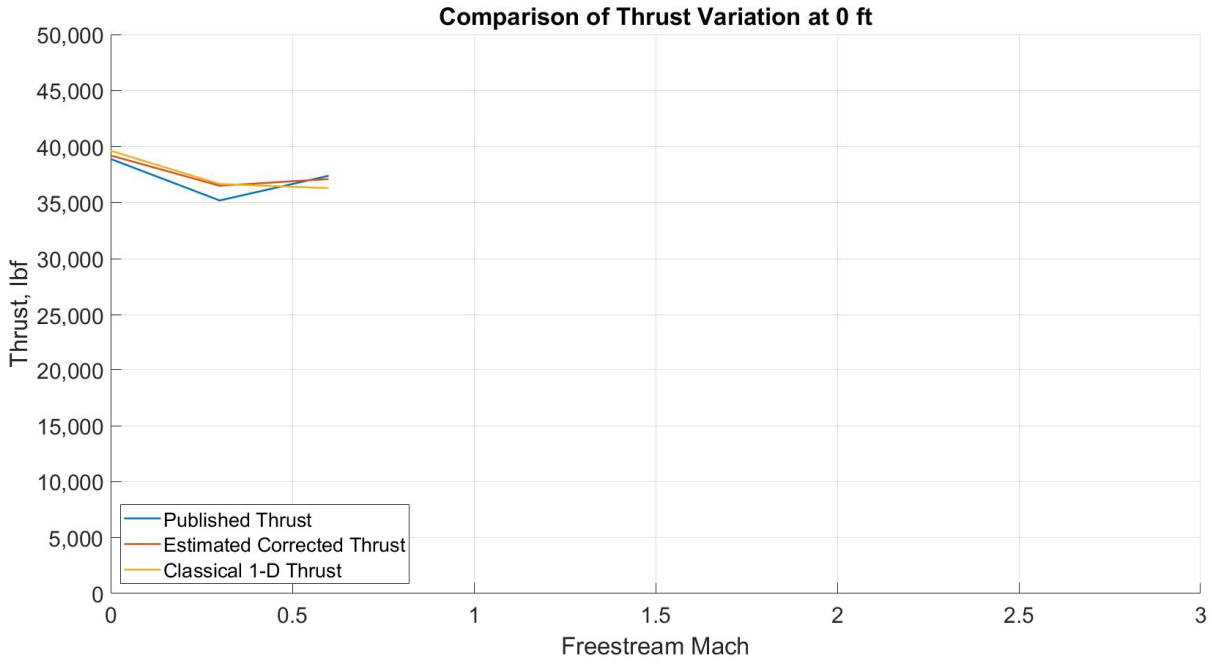

Fig. 14 – Comparison of Thrust at Sea Level

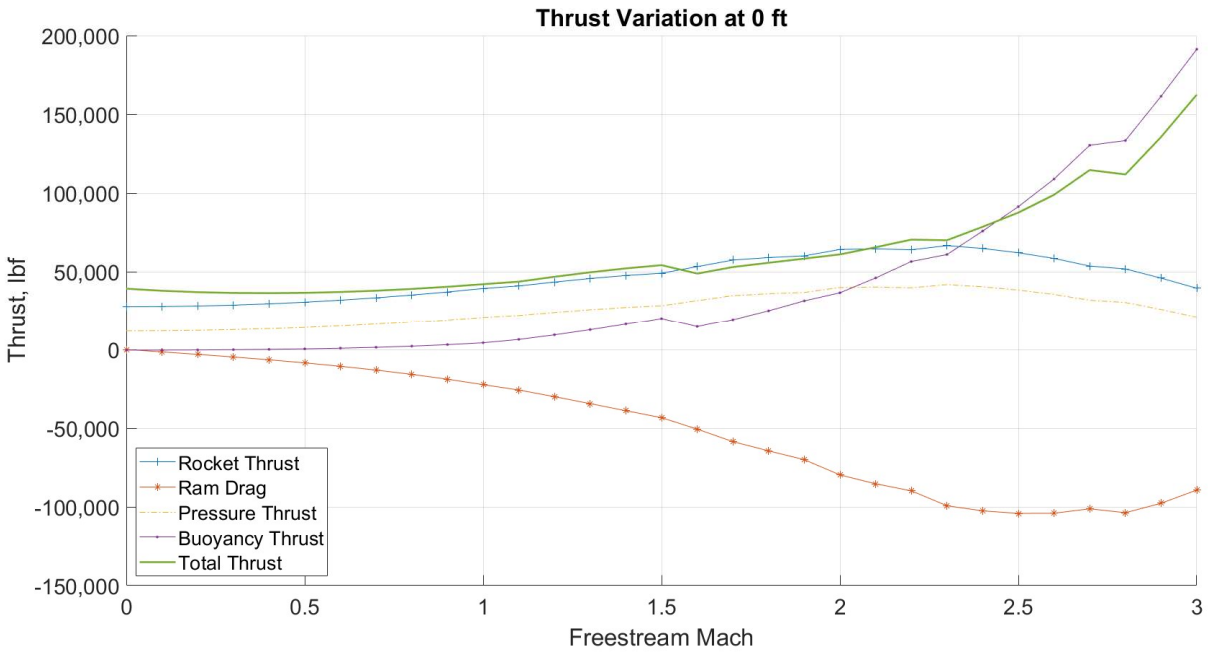

Fig. 15 – Component-wise Distribution of Thrust at Sea Level

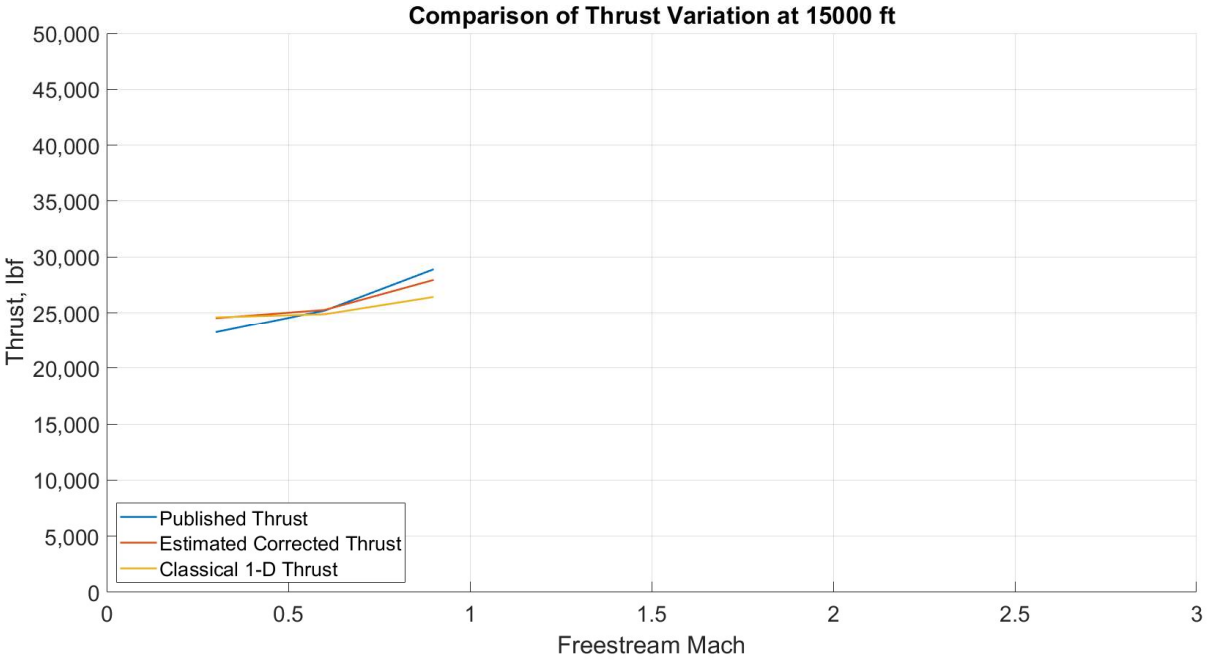

Fig. 16 – Comparison of Thrust at Altitude of 15,000 ft

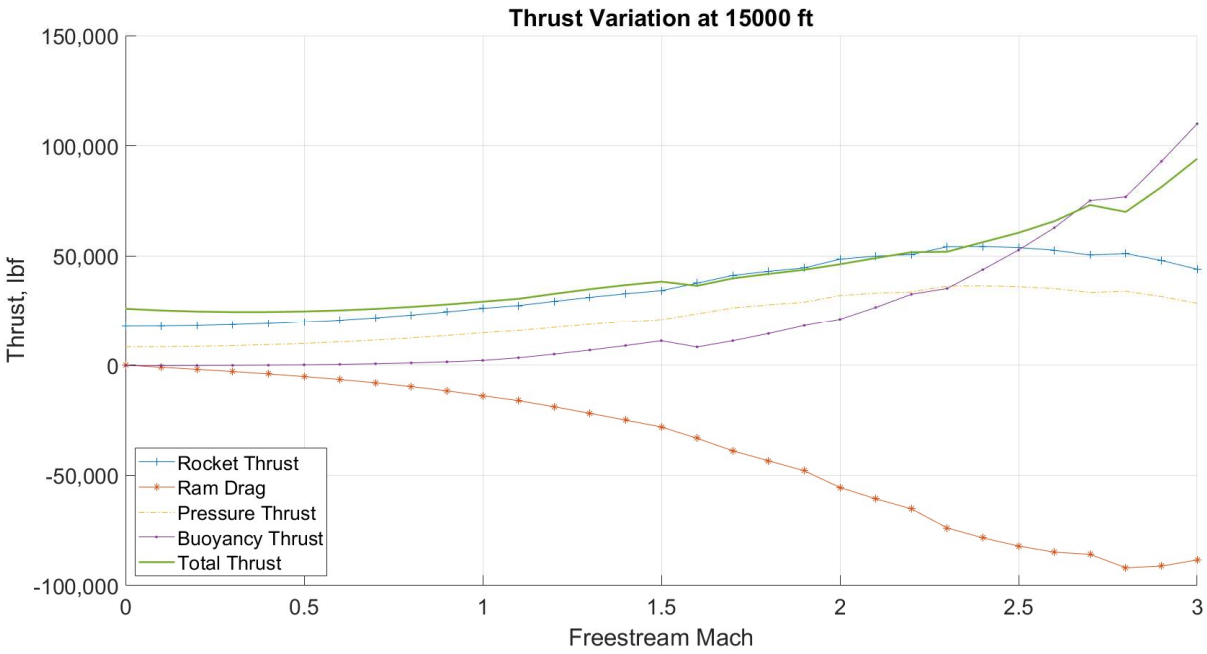

Fig. 17 – Component-wise Distribution of Thrust at Altitude of 15,000 ft

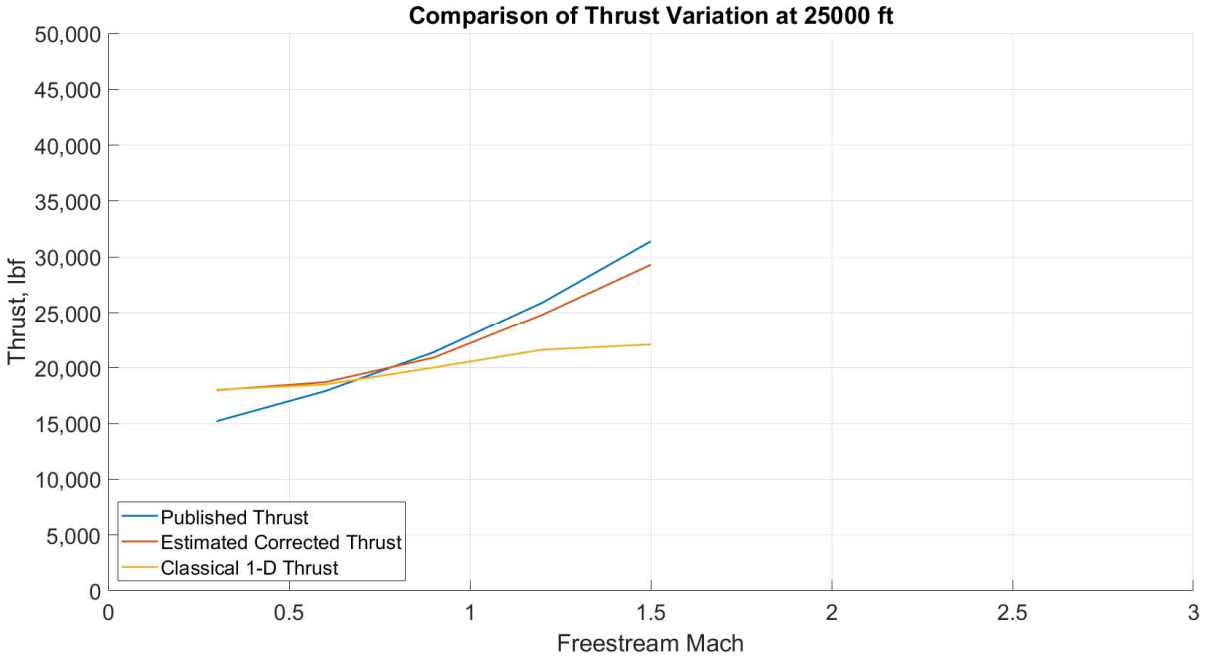

Fig. 18 – Comparison of Thrust at Altitude of 25,000 ft

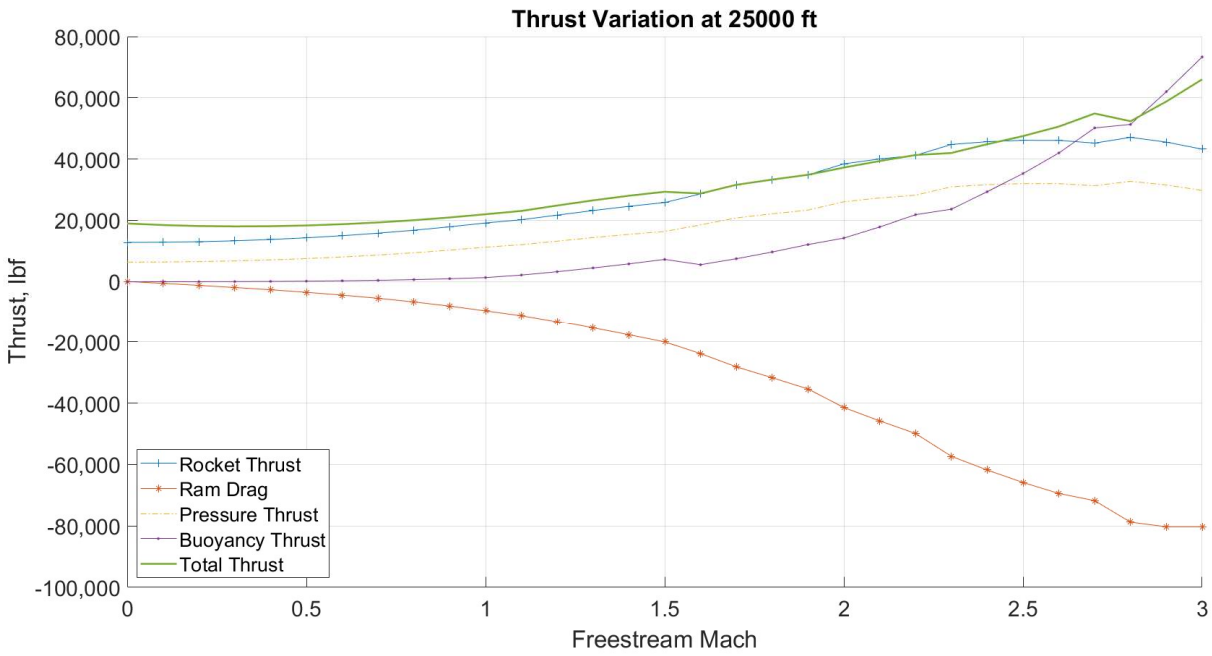

Fig. 19 – Component-wise Distribution of Thrust at Altitude of 25,000 ft

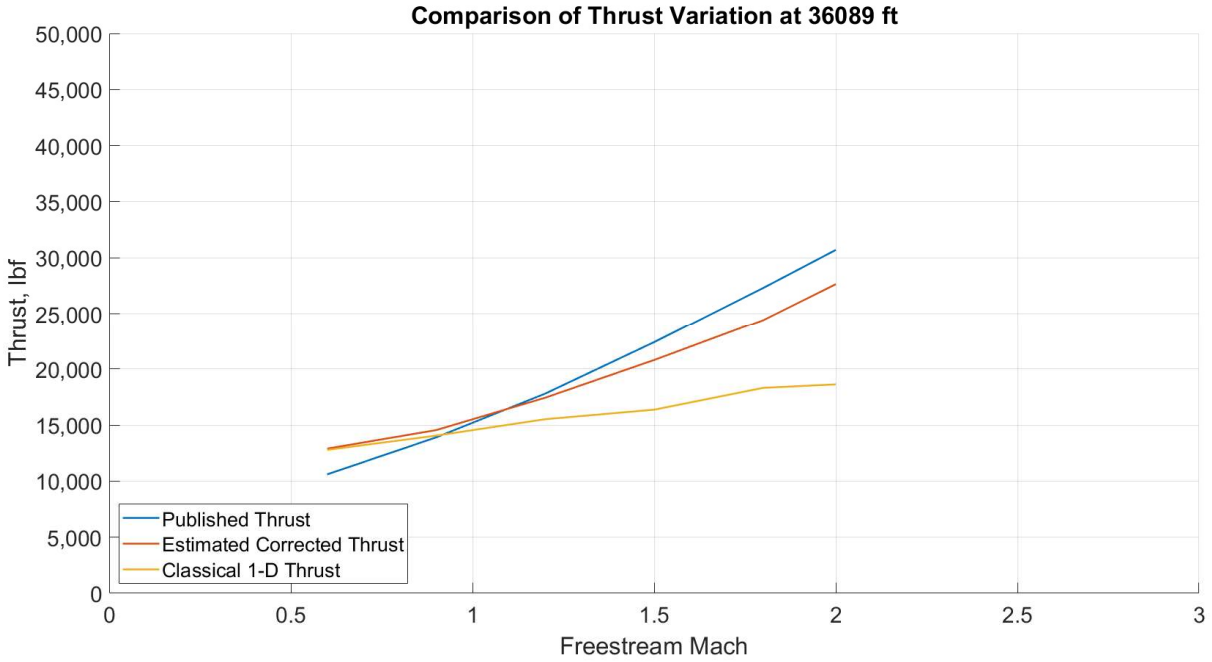

Fig. 20 – Comparison of Thrust at Altitude of 36,089 ft

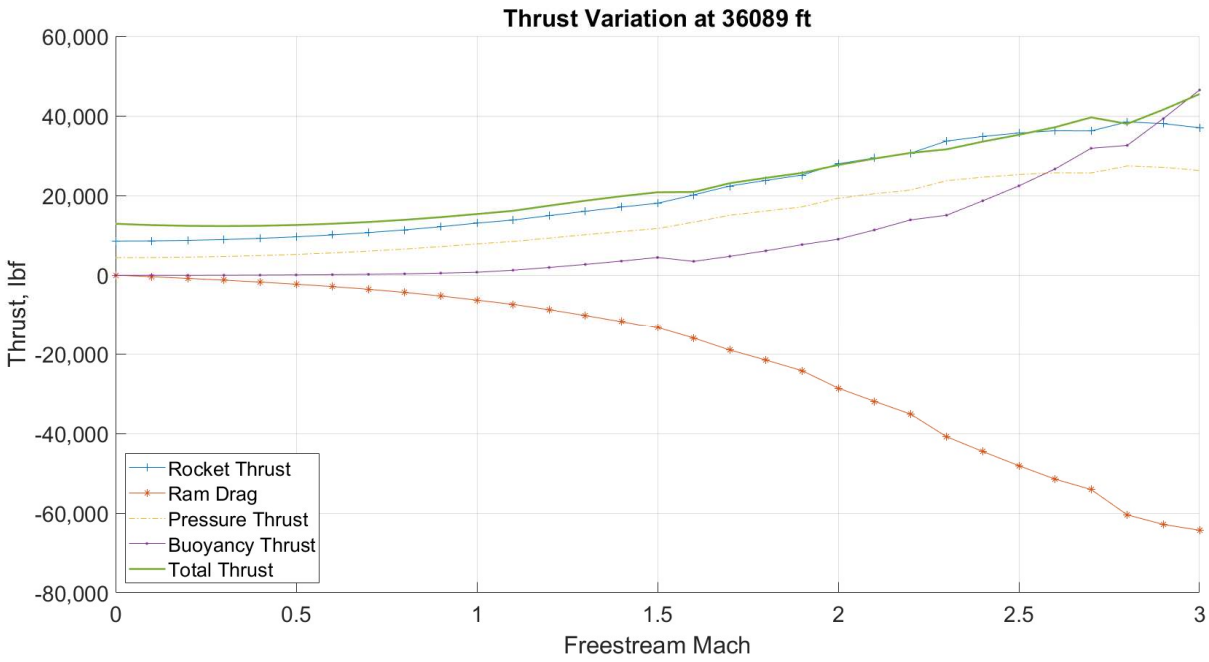

Fig. 21 – Component-wise Distribution of Thrust at Altitude of 36,089 ft

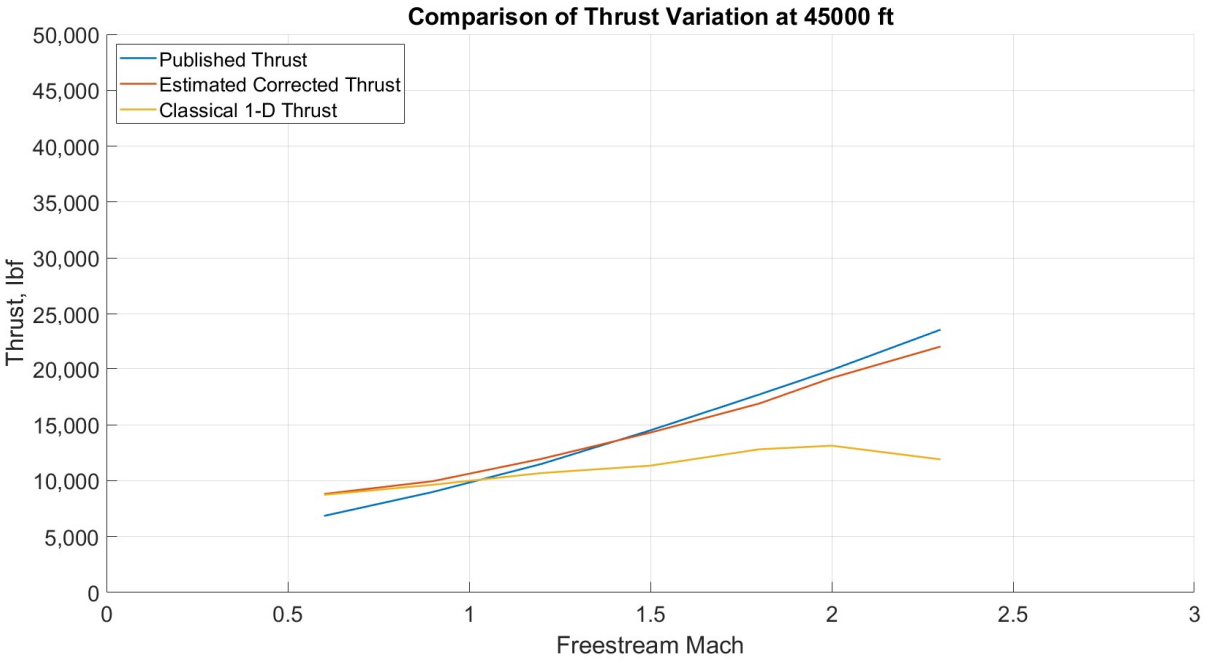

Fig. 22 – Comparison of Thrust at Altitude of 45,000 ft

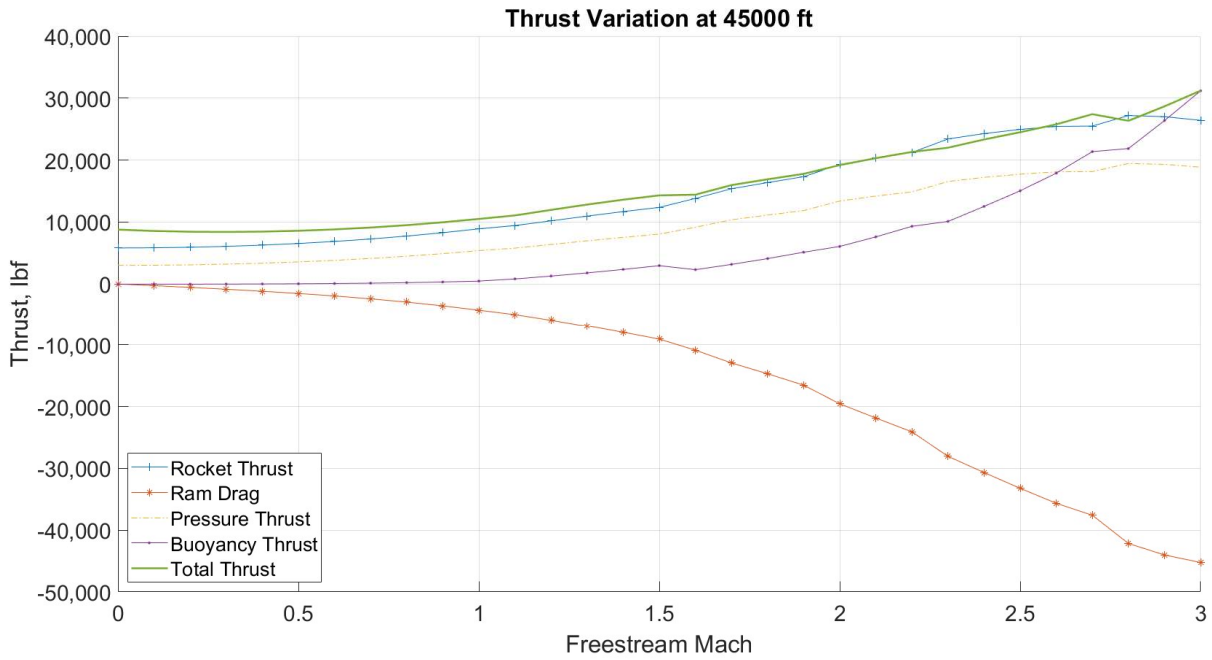

Fig. 23 – Component-wise Distribution of Thrust at Altitude of 45,000 ft

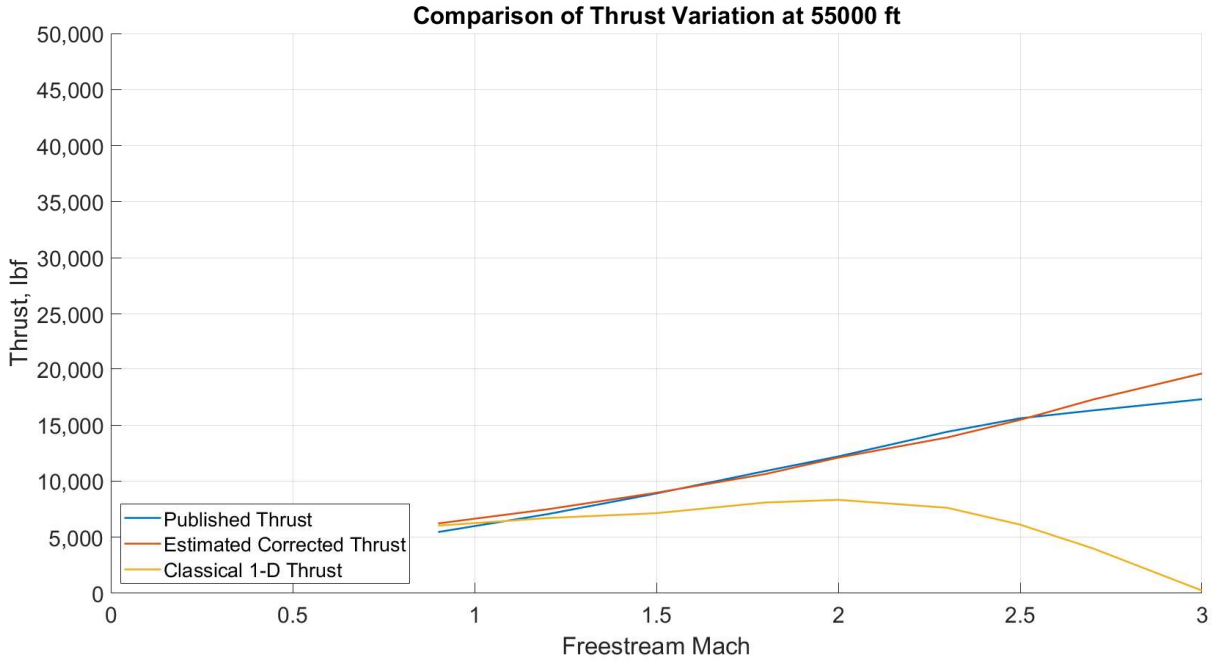

Fig. 24 – Comparison of Thrust at Altitude of 55,000 ft

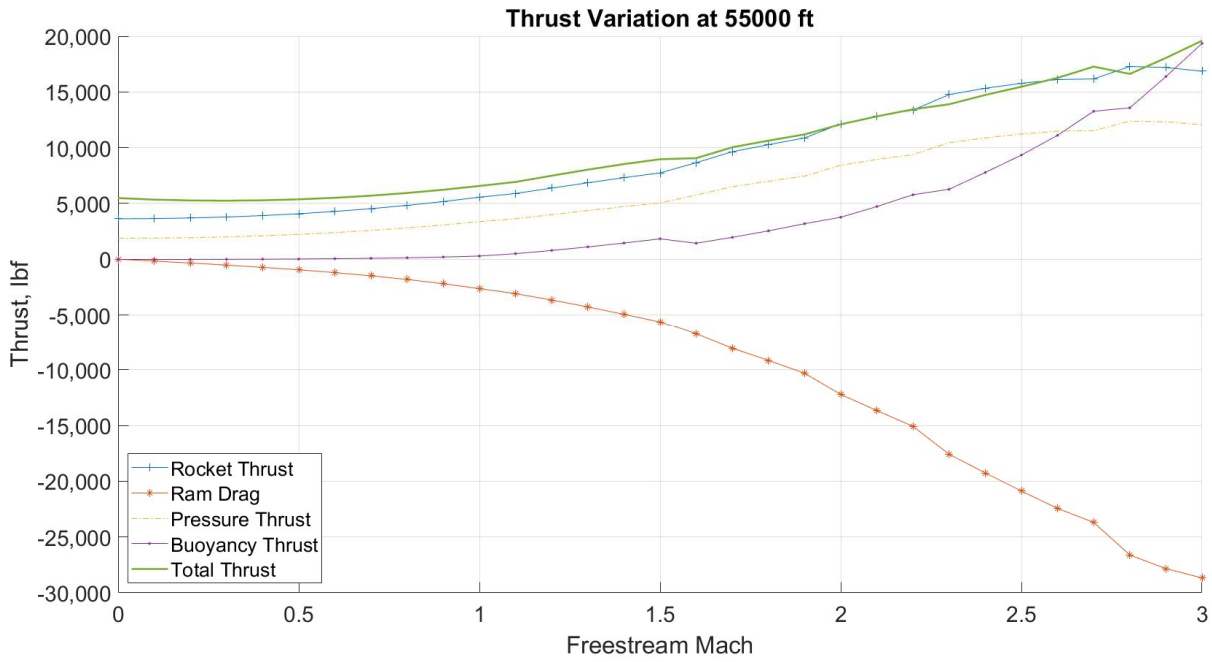

Fig. 25 – Component-wise Distribution of Thrust at Altitude of 55,000 ft

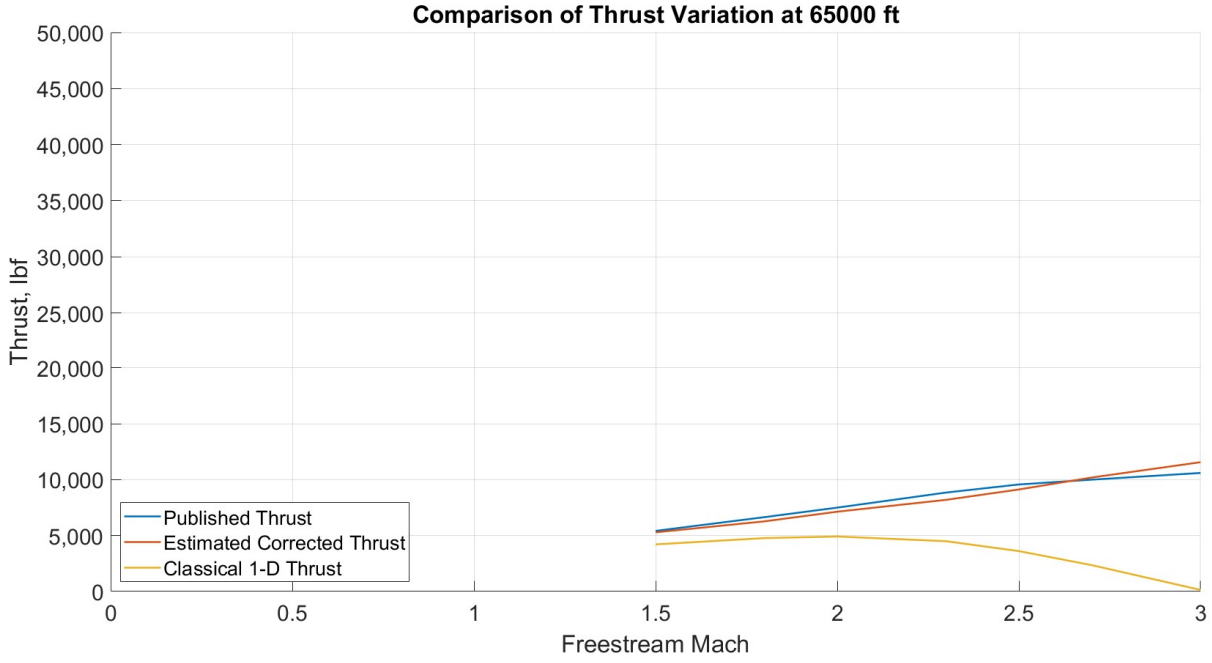

Fig. 26 – Comparison of Thrust at Altitude of 65,000 ft

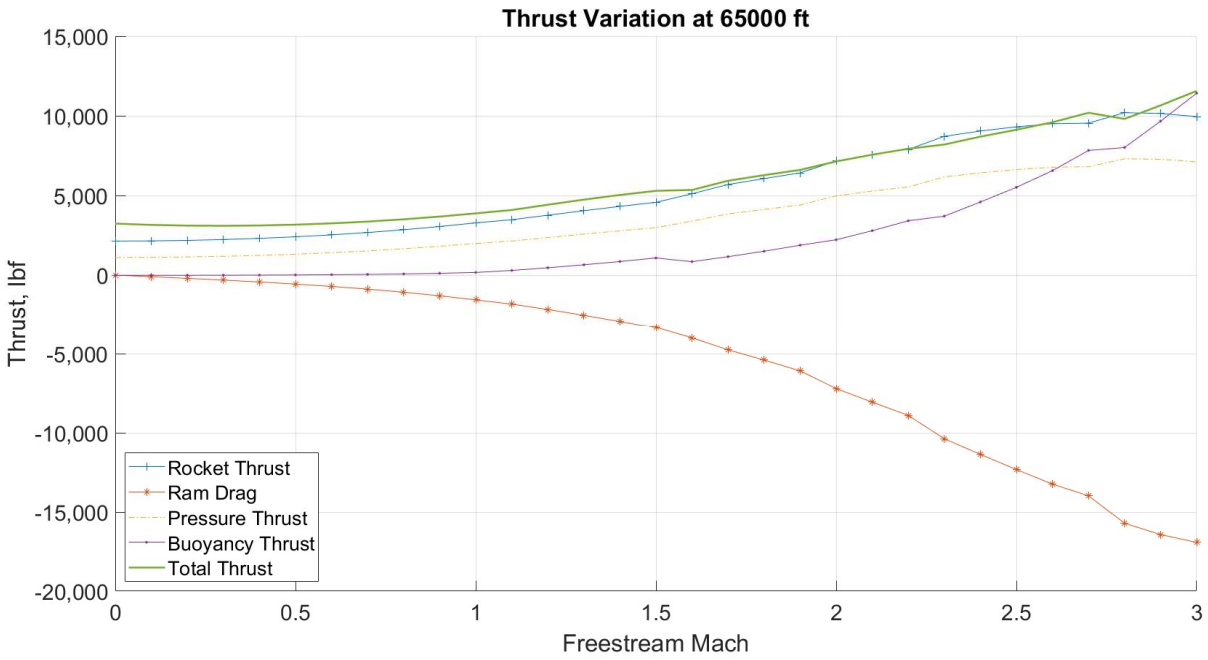

Fig. 27 – Component-wise Distribution of Thrust at Altitude of 65,000 ft

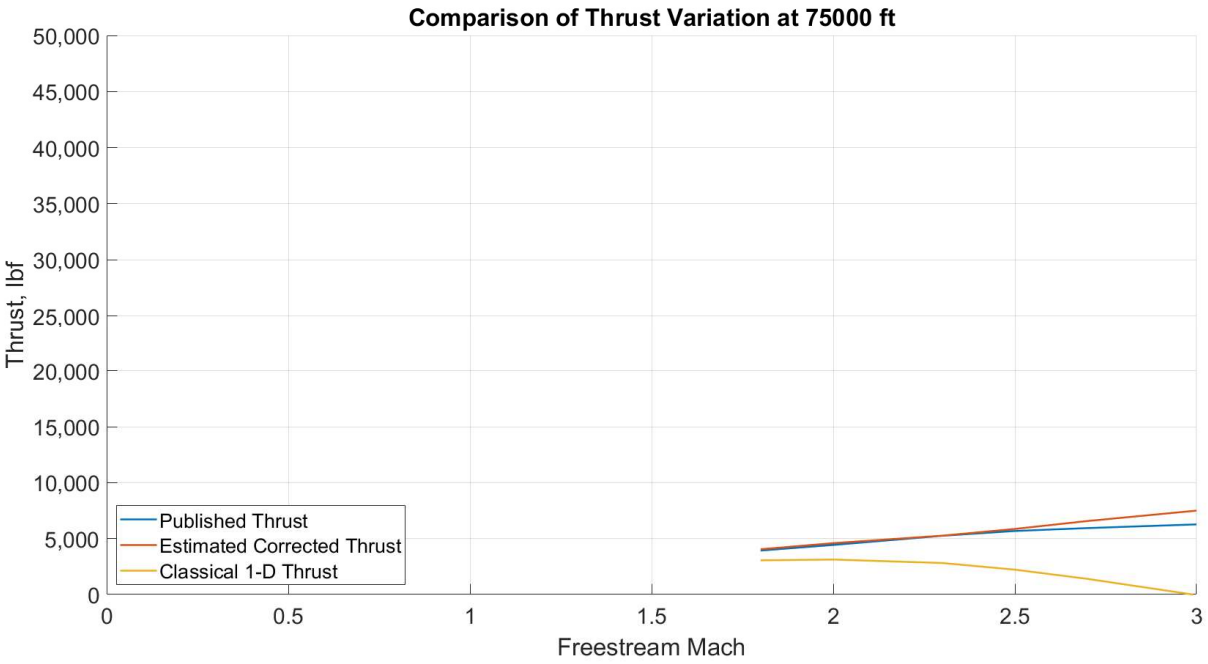

Fig. 28 – Comparison of Thrust at Altitude of 75,000 ft

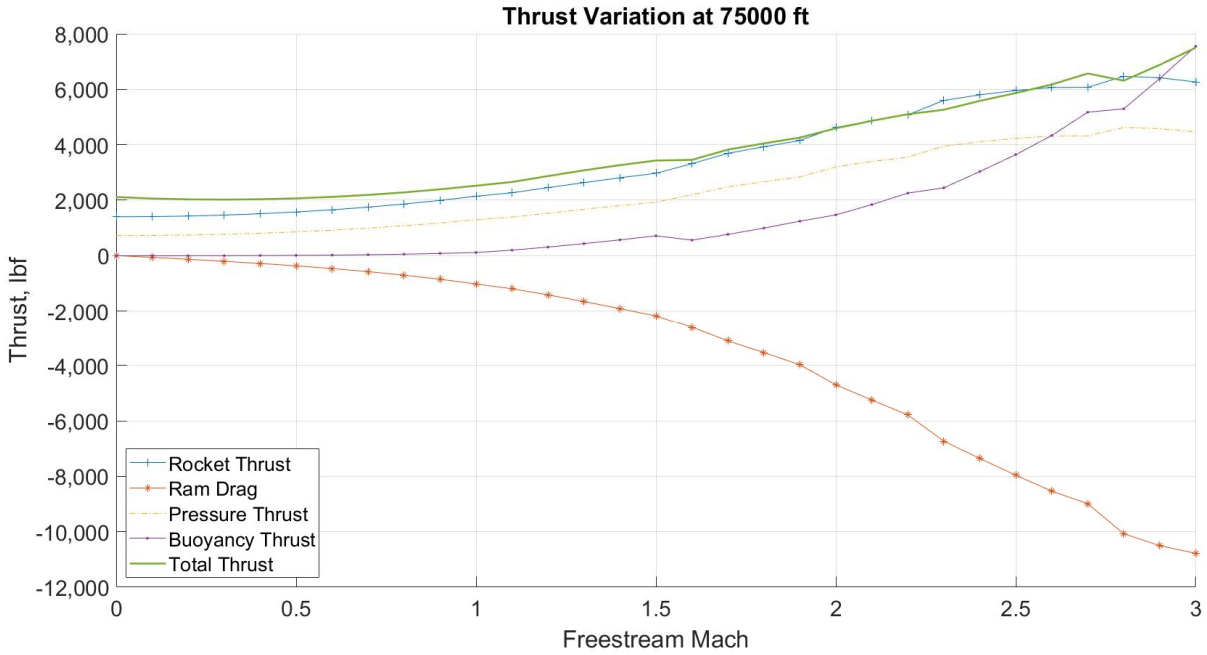

Fig. 29 – Component-wise Distribution of Thrust at Altitude of 75,000 ft

Upon closely observing the component-wise distribution of thrust figures, one may observe that the buoyancy force starts of from negative and then slowly crosses over to the positive side once the flight speed becomes more than the fan speed. Moreover, a slight decline near Mach 1.5 is observed due to the fact that a conical shock is observed from this point onwards which tends to slightly lower the buoyancy pressure generated across the entire inlet face, and hence the reduction.

Moreover, the difference between the 1-D classical and newly estimated thrust might not seem to be much bigger in subsonic region, but as can be clearly viewed from the results above, when the freestream Mach number crosses the sonic speed, the impact due to buoyancy is one of the leading contributor in net thrust generation of a turbojet engine. It also becomes clear that if the buoyancy force was not considered, then in that case the classical 1-D thrust equation would yield a negative thrust value as is observed at higher supersonic speeds, which would make it unreasonable for the aircraft to move forward. Moreover, it would have led to over design of the engine to produce significant positive thrust to propel the aircraft forwards, which would be careless wasting of resources.

The Table 2 following this, shows contribution of various components of thrust at various flight scenarios as obtained from executing the previously mentioned analysis method. The conditions are a not true representation of the aircraft position, but a strong guess based on the flight operation studied in the companion paper [24]. The values in the table are computed at “Military” (i.e., un-augmented thrust at the design OPR and TIT).

Table 2 Contribution of each component of thrust towards net thrust at different flight scenarios.

Freestream Mach	*Altitude (ft)*	*Ram Drag (% of Net thrust)*	*Rocket Thrust (% of Net thrust)*	*Pressure Thrust (% of Net thrust)*	*Buoyancy Thrust (% of Net thrust)*	*Net Thrust (lbf)*
0	0	0	70.66	30.38	-1.05	39,212.86
0.3	0	-13.11	78.72	34.80	-0.41	36,513.65
0.4	15,000	-16.18	77.86	38.21	0.11	24,530.73
0.8	25,000	-33.45	83.62	46.83	2.99	20,015.02
0.9	36,089	-36.06	83.51	49.17	3.37	14,548.01
1.1	36,089	-45.55	85.64	52.29	7.61	16,142.30
1.2	45,000	-49.18	85.24	53.30	10.63	11,955.37
1.5	45,000	-63.34	86.44	56.23	20.66	14,297.19
1.8	55,000	-86.16	96.55	65.72	23.88	10,633.32
2.1	55,000	-106.71	100.01	69.83	36.86	12,805.61
2.5	65,000	-135.04	102.03	72.61	60.40	9,124.11
2.7	75,000	-136.81	92.403	65.67	78.73	6,570.49

VIII. Conclusion

It becomes clearer from observing the previously displayed figures that the turbojet engine developed here with consideration of the inlet buoyancy force performs similarly to the engine for which the data has been presented in the report. With this approach, a successful propulsion database can be created, which could be used to truly understand the performance of the aircraft in supersonic condition using energy-maneuverability theory.

Moreover, the slight differences in the value are due to the fact that the dimensions used to define the bounds of the turbojet engine might be different from those that define the actual engine. Moreover, the Mach numbers used as design parameters for different sections in the turbojet engine are the best guesses from the study of different engines of the same era. It is also important to understand that most supersonic engine developed during the legacy era were used for military purpose unlike the GE4 engines, which were specifically designed to thrust commercial supersonic airliner.

Moreover, the buoyancy thrust estimated and then used to calculated net thrust might vary since, the inlet in this case was designed such that it would perform external compression and all the shocks will be sitting on the cowl lip with diffusion occurring once the throat is crossed. The consideration of diffusion is very important in designing the inlet, since it helps to roughly approximate Mach number needed before diffusion, which would be the Mach number after the normal shock for design condition. The method mentioned above was primarily used for designing the supersonic inlet for this case. It could also be the case that the diffusion ratio for GE4 engine be different than the one used for this case. Moreover, the Turbine Inlet Temperature and Static Pressure Ratio also were not available and hence were approximated based on preexisting knowledge of engines of the same era. Along with factors such as bypass leakage and component efficiencies, there could be many other contributing factors that might be the difference between the calculated and published thrust values.

All in all, one of the objective of this work was to display the amount of contribution that the buoyancy force provides to the net thrust. Based on the readings observed in Table 1, the buoyancy force is one which cannot and should not be neglected during conceptual design and analysis of the aircraft irrespective of whether an aerodynamicist or a propulsion engineer accounts for it in the pre- and post- analysis data.

Acknowledgements

This manuscript derives from work Mr. Chaudhari performed in partial fulfillment of the degree requirements for obtaining his M.S. in Aerospace Engineering from Arizona State University. All design analysis on this unfunded project was completed at Arizona State University.

References

[1] Trautvetter, C., "Gulfstream Continues Supersonic Business Jet Research," AIN Online [online periodical], URL: https://www.ainonline.com/aviation-news/business-aviation/2016-12-06/gulfstream-continues-supersonic business-jet-research [cited 6 November 2017].
[2] Reed, D., "The High Price Of High Speed: At $120M Each, Can Aerion Sell Enough Supersonic Jets To Earn A Profit?," Forbes [online periodical], URL: https://www.forbes.com/sites/danielreed/2015/11/19/the-high-price-of-high-speed-at-120-million-each-can-aerion-sell-enough-as2s-to-earn-a-profit/#45f7b952115c [cited 6 November 2017].
[3] Shaban, H., "A start-up says its new planes will get passengers from New York To London in 2.5 hours," The Washington Post [online periodical], URL: https://www.washingtonpost.com/news/innovations/wp/2017/06/20/a-startup-says-its-new-planes-will-get passengers-from-new-york-to-london-in-2-5-hours/?utm_term=.02cdf0feceaf [cited 6 November 2017].
[4] The Concorde Makes its final flight – History, 2020. [Online] Available: https://www.history.com/this-day-in-history/the-concorde-makes-its-final-flight
[5] Dickman, C. & Takahashi, T.T., "Engine/Inlet Matching for Supersonic Aircraft Design," AIAA 2016-0771, 2016
[6] Palma, R.M. & Takahashi, T.T., "The Effects of Supersonic Inlet Topology on the Installed Performance of Turbofan Engines," AIAA 2016-3563, 2016.
[7] Cleary, S. & Takahashi, T.T., "The Effects of Fixed Conical Spike Inlets on the Performance of Higher Bypass Ratio Engines," AIAA 2018-3836, 2018.
[8] NPSS, Numerical Propulsion System Simulation, Software Package, Ver. 2.8, Ohio Aerospace Institute,
[9] Ball, W. H. & Hickcox, T. E, "Rapid Evaluation of Propulsion System Effects. Volume I," TECHNICAL REPORT AFFDL-TR-78-91, VOLUME I, July 1978.
[10] Ball, W. H. & Atkins, R.A., Jr., "Rapid Evaluation of Propulsion System Effects. Volume II – *PIPSI* Users Manual," TECHNICAL REPORT AFFDL-TR-78-91, VOLUME II, July 1978.
[11] Hickcox, T. E., Atkins, R.A., Jr. & Ball, W.H., "Rapid Evaluation of Propulsion System Effects. Volume III Derivative Procedure User's Manual," TECHNICAL REPORT AFFDL-TR-78-91, VOLUME III, July 1978.
[12] Ball, W.H., "Rapid Evaluation of Propulsion System Effects. Volume IV – Library of Configurations and Performance Maps," TECHNICAL REPORT AFFDL-TR-78-91, VOLUME IV, July 1978.
[13] Concorde – Celebrating an Aviation Icon, [Online] http://www.concordesst.com/powerplant.html
[14] Costello, J. & Hughes, T., The Battle for Concorde, Compton Press Ltd, Salisbury, UK, 1971.
[15] Takahashi, T.T. & Cleary, S., "Inlet Diffusor Buoyancy – An Overlooked Term in the Thrust Equation," AIAA - 2020-2642, 2020.
[16] Hill, P.G. & Peterson, C.R., Mechanics & Thermodynamics of Propulsion, Addison Wesley, New York, 1991.
[17] Numbers, K.E., "Hypersonic Propulsion System Force Accounting', AIAA-91-0228, 29th Aerospace Sciences Meeting, Reno, Nevada, 1991.
[18] Dowling, S., "The American Concordes that never flew," BBC, 2016. [Online]. Available: https://www.bbc.com/future/article/20160321-the-american-concordesthat-never-flew.
[19] Bush, R.M.,"Boeing Model 2707 - Model Specification, Supersonic Transport Development Program, Phase III," The Boeing Company - Supersonic Transport Division, AD 827442, 1968.
[20] Brady, K.G. "Boeing Model 2707 - System Engineering Report, Supersonic Transport Development Program, Phase III Proposal," The Boeing Company, AD 804721, 1967.
[21] "Engine Performance Report - GE4/J4C, Commercial Supersonic Transport Engine Proposal," General Electric - Flight Propulsion Division, Vol. E-IV GE4/J4C", DTIC AD 377961, 1964.
[22] "US Standard Atmosphere 1962," NASA, AD 659893, 1962.
[23] MIL STD 5008B
[24] Chaudhari, B. & Takahashi, T.T., "Reassessing the B2707-100 Supersonic Transport Aircraft," AIAA-2022-0776, 2022.
[25] Wilkinson, P.H., Aircraft engines of the World: 1970, Paul H. Wilkinson, New York, 1970.
[26] Anderson, J.T., "How Supersonic Inlets Work: Details of the Geometry and Operation of the SR-71 Mixed Compression Inlet," Lockheed Martin Skunk Works.
[27] Benson, T., "Normal Shock Waves," NASA Glenn Research Center, 2014. [Online]. Available: https://www.grc.nasa.gov/www/BGH/normal.html.
[28] Dahm, W.J.A., MAE 563 - Aircraft Propulsion, Ira A. Fulton Schools of Engineering, Arizona State University, Fall 2019.